Stringham, R. *Ejecta Sites and DD Fusion Events*. in *APS March Meeting*. 2006. Baltimore, MD.

Ejecta Sites And DD Fusion Events

Roger S. Stringham
PO Box 1230, Kilauea, HI USA

ABSTRACT

A cavitation-produced jet that implants a target foil at high impact velocities produces foil damage shown in color and SEM, scanning electron microscopy, photos. The work here dates from 1989 to 2001 and was produced in several different reactors, target foils, and frequencies. The result of high density pinched implantation of D^+ and e^-, deuterons and electrons; plasma is a D^+ cluster. The implant occurs in a picosecond time frame with a creation of D^+/Pd, in a 100/1 ratio of an initially electron free D^+ cluster with a diameter in the order of a hundred nm. The mobile e^- react with D^+ and surround the D^+ cluster with D. DD fusion events occurring in the transient high-density cluster produce a gamma free heat pulse. The heat pulse reaches the lattice surface in a nanosecond expelling the vapor/liquid foil and products as ejecta. The ejecta sites are easily seen in SEM photos and are counted and plotted as MeV DD fusion events. The results have been interpreted as DD fusion events that increase in energy as they decrease in frequency (counts) exponentially.

INTRODUCTION

Experiments were performed over the time period, 1989 to 2001, using a number of different devices that followed the basic design and reactor configuration of the Mark I that I put into use in1989. All reactors used a thin reaction volume of cavitating D_2O driven by one or two piezos where the parameters of temperature, pressure, and acoustic input are controlled. The 20 KHz Mark I and Mark II apparatus, the 40KHz Mark III static and dynamic apparatus, and the 42 KHz Mark IIII were similar. Mark I & II reactors were driven by an acoustic horn and Mark III, IIII, and 5 were driven by opposing dual acoustic stacks. Bill Snook machined five of these devices to my specifications. Also the Mark 5, a dual stack apparatus that ran at 46 KHz, was machined by Scott Little, also to my specifications. The Mark 5 piezo oscillator was designed by Kip Wallace [1]. The Mark 5 was suitable for use in the mass flow calorimetry system at SRI with input and assistance from Fran Tanzella and Michael McKubre. During the cavitation experiments more than 50 target foils were exposed to various temperatures, pressures and acoustic inputs. The sonofusion experimental sites were also varied. The following short list of experimental sites (PS Consulting, EQuest, SRI*, LANL*, and First Gate) all produced similar target foil damage when analyzed by SEM. George Chambers of the NRL was present during these experiments, thanks to David Nagle.

This is a best guess of sequential transient events, some of which may overlap in their time frames, that originate from acoustic created collapsing transient cavitation bubbles, TCBs, at a frequency of 20 to 50 KHz. This paper is a compilation of experimental work undertaken over a 12 year period that have been assembled to give a better understanding of a unique process. The

ideas expressed here are my best choice for a path that produces DD fusion events including a TCB collapse, a target implantation, and a heat pulse ejection of target material. I would like to point out that what follows is not the only path. My experimental work with piezo driven acoustic fields produced in thin piezo driven reactors with target foils, presents a reasonable path for fusion events in the foils. If one accepts that the transient high density environment of implanted D^+ as the source of DD fusion, where captured gases, ^{4}He and T, [2] from the reactor are measured, is proof of fusion events, then what follows is an alternate path for this fusion product. An alternate path [3] for fusion energy dispersal exists in the form of heat instead of the 24 MeV gammas. During the measurement for gammas none were found in experiments where fusion products were produced (^{4}He and T). I hope that the ideas, graphs, and photos result in a better understanding of TCBs, their jet formation, implantation into targets, and the extremely fast time-frame for events that can result DD fusion. These fusion events occur within the very dense D^+ target foil implantation (10^{25} ions/cc). A fusion event in the target lattice occurs before deuteron diffusion and coulomb repulsion reduces the implant density of the deuteron clusters. And finally, the accompanying DD fusion heat pulse, that breaks the foil surface, ejects some of the target foil as vapor or liquid leaving behind an ejecta site in a target foil. The mass and velocity of the ejecta is energy in the heat pulse ejecta sites and that of the DD fusion event. The ejecta sites are pictured in the SEM photos.

Note: The pseudo adiabatic collapse of the cavitation bubble follows the rate of change of the average bubble radius, dr/dt, which is elliptical phenomenologically [8,10]. The average rate of bubble radius collapse has been determined experimentally by a number of laboratories but assumes a spherical bubble collapse during this process. The assumed bubble symmetry is only an ideal but in reality the collapsing bubble pulses and oscillates in the cavitating chaotic environment in the reactor. Much of the bubble physics for the multi-bubble system I used has been extrapolated from the single bubble experiments. A good informational overview on today's bubble physics is found in Reviews of Modern Physics, volume 74, April 2002; Michael. P. Brenner, Sascha Hilgenfeldt, and Detlef Lohse [4].

The acoustic input into a reactor produces millions of bubbles in one cc of water where only those bubbles with the initial resonance size will couple in an isothermal rapid growth process and become TCBs. This process selects a narrow range of energies – bubble sizes - for the TCB and this leads to a narrow distribution of bubble energy densities during the collapse process. The energy density in the final stage of the bubble collapse depends on the reactor's running parameters and resonance frequency of the piezo-reactor. The running parameters for the TCB's initial and final energy density during the growth and collapse process are temperature, external pressure, and acoustic input. All of these determine final energy density of a TCB. The TCB sonoluminescence, SL, [5] and the evidence of products from decomposition of long term cavitating water produce steadystate concentrations of H_2 and HOOH [6] and are evidence of a few picoseconds of SL and a TCB plasma presence [7]. These products will be found in all combinations of hydrogen isotopes in water molecules. The extension of this process is linked to the transfer of the TCB plasma to the jet where it is further compressed by the high velocity sheath electrons (Boit – Savart law). This plasma compression force tends to kink and destroy plasmas in microseconds and is a major problem in the Tokamak type of hot fusion plasma reactors. The advantage of the TCB and its accelerating cavitation jet is the short picosecond time frame that squeezes the jet's contents [8]. The time frame for TCB jet squeeze is much too short for any disruption, via a kink in the jet acceleration of its plasma.

The TCB jet plasma implantation of D^+ into a target foil is a transient phenomenon and does not appear to load deuterium into the lattice of a Pd foil. During a visit to Ed Storms' lab in 1998 Santa Fe, NM, gravimetric experiments showed that no weight change was found in a target foil before and after cavitation exposure. The deformation of a Pd target foil in x-ray diffraction analysis by NRL, under the direction of George Chambers, shows a change in the lattice that corresponds to that of PdD. These measurements were made on Pd100μm foils months after removal from the reactor allowing plenty of time for D to diffuse from the Pd foil. The conclusion is that there is no measurable loading of D into a Pd lattice and the deformed lattice remains in its deformed state after diffusion of D. This is an unresolved problem. The heat pulse generated in a DD fusion event after a jet implantation of D^+ removes all species in the local environment via ejecta. As the heat pulse travels to the foil surface, about a nanosecond, all species present (D, D^+, Pd, ^{4}He, DT, and etc.) in the growing vapor/liquid Pd heat pulse located initially in the implant cluster are ejected into the cavitating D_2O. The ^{4}He that would normally be locked in the Pd lattice and T which will slowly diffuse are immediately freed for gas phase MS analysis.

TARGET FOIL DAMAGE

The target foil damage observed at 20 to 46 KHz are similar and treated as being the same. The targets in cavitating water (water being light or heavy) will sustain continuous damage to the surface and over time will destroy the foil. The SEM photos capture the condition of the surface's progressive damage at the moment of the foil's removal from the cavitating environment. The target surface is continuously heated and cooled during its cavitation exposure. The damage to the target foil is divided into three parts. The colored and SEM photos of these foils reveal details of damage via three distinctly different damage mechanisms (I) bombardment, (II) implantation, and (III) fusion. I) The bombardment by 1 μm Pd particles that are accelerated into the target foil via the TCB plasma jet to form 100μm impact craters are shown in SEM photos. II) The SEM examination of surface features of the foil indicate that during implantation a polishing of the foil surface by the larger ions (Ar and O) that do not penetrate into the lattice takes place. The D^+ and e^- do penetrate into the lattice forming D^+ clusters and local high concentrations of mobile e^-. III) The damage to foils via the DD fusion events tens of nanometers deep in the target foil produce a heat pulse that escapes from foil surface as the volcanic-like ejecta producing ejecta site holes in the target foils. These foil damage activities I, II, and III continuously rework the target metal surface during the time of cavitation exposure. All foils are exposed to TCBs where the bubbles exist for one acoustic cycle before violently collapsing. This requires a high acoustic input with respect to the water temperature and external pressure of argon gas [11].

Before discussing the jet impact system I want to point out an unusual micro-meteor effect that has been observed. This is damage mechanism 1) figure 1; bombardment of the target foil by micron size metal particles is an observed phenomenon via SEM. When one considers the billions of bubbles produced per second this micro-bombardment is a rare occurrence, but it emphasizes the fact that the cavitation jet is a micro deuteron accelerator. In rare situations a particle trapped in the TCB interface is accelerated by the jet into the target. During a cavitation bubble collapse, once in awhile a free particle in the order of 1 μm, is captured by surface tension between the bubble's liquid and vapor phase. See the1 μm spheres in figure 2. The bubble's interface, with the particle, is accelerated into the collapsing bubble jet. I believe the high velocity jet, with the surface tension locked particle in the interface, is acting as a particle

accelerator and impacting the target foils with these relatively large particles at micro meteor velocities. There are some SEM photos that clearly show 100μm impact craters found in the cavitation exposed Pd target foils. The SEM photos show evidence of such a bombardment.

Figure 1 shows a crater impact in a 100 μm thick Pd foil, from Johnson Matthey Co., produced after exposure to cavitating D_2O, in the M 5 reactor in the flow through calorimeter at SRI. The 1999 SEM FE photo by Jane Wheeler of Surface Technology was one of many good photos. The crater diameter and depth was what would be expected from a high velocity 1 μm particle impact similar to that of a micro meteor. The SEM photo, figure 2, of a 100μm thick Ag foil, from JM produced after exposure to cavitating D_2O, in a M III reactor shows a debris field of 1 μm particles that condensed in D_2O environment on the foil from a vent ejecta site. Similar 1 μm spheres are found in exposed Pd foils. Figure 2, 1998, photo is from Lee Instruments, based in San Leandro, CA. Figure 3 is the same Ag foil and same photo source as figure 2 and shows a large vent site 5μm in diameter and the view into the vent site showing the condensed Ag 1 μm spherical surface bumps on the walls of the ejecta site from the heat pulse ejecta.

The SEM FE photo of a Pd foil in the M III reactor of a cavitation exposed surface is pictured in figure 4. The 1 μm inset shows the more common smaller Pd foil vent sites . Figure 4 is typical of the 0.01×25 cm^2 cavitation exposed Pd foil top and bottom surface.

The 1 μm particles originate from ejecta (see figure 6A 3'→3) produced by a fusion generated heat pulse in the target foil. These particles are common, as can be seen in many SEM photos, where the 1 mμ spherical particles are stuck on the sides of ejecta sites via a Pd vapor/liquid involved in a condensation process that occurs shortly after a jet implant and the following fusion and heat pulse.

It is interesting to note that these impact kinetic energy, KE, systems can be scaled to match large terrestrial (land and water) and extraterrestrial meteor impact systems. See figure 5. The similarities between micro-meteor impacts on the surface meteors (space vehicles) and the impacts seen in target foils are very close. The high velocity target impacts give support to the velocities of the bubble interface passed on to the bubble or plasma jet contents in the form of a deuteron accelerator.

IMPLANTING PLASMA

Implantation of D^+ and e^- jet contents into the Pd lattice are different from an atomic ion beam. The plasma implant is an especially dense plasma implant, 10 orders higher. With the energy of 100ev for the D^+ in an ion beam the impact range into a target foil is less than 10^{-10} m (less than the radius of a Pd atom) [14]. The D^+s are part of a dense plasma and a collection of implanted particles in a target foil (D, D^+ and e^- particles) that are interactive with each other. The range of a D^+ in the target is much more than that of a D^+ in ion beams [14]. The D and D^+ exist sharing e^- associations in the jet plasma as the jet plasma impacts the target foil. D^+ and e^- will range deep into the lattice, with the characteristics of a liquid. The penetration of D^+ into the lattice is related to its collision cross section of the target and the Debye screening distance. Implanting D (the unionized D in the dense low temperature plasma) may or may not be part of the implant when stripped of its e^- at target impact.

The collapsing TCB forms, from the bubble's plasma contents in its final stage of collapse [12], a high density low energy plasma jet. This high velocity jet implants its deuteron and

electron content into the target foil. The heavier and much larger ions Ar and O are left behind due to their high (mass and volume)/(charge) ratio and do not enter the foil lattice. The collision cross-section at the foil surface of D^+ and e^- is low compared to Ar and O ions. I believe Ar and O ions are effectively stripped from the impacting plasma. Note that the TCB jet implantation is not an efficient process as most of these jets will deposit their contents into the water where the plasma constituents recombine into their original water form [8]. The expected energy of implantation of the high-density plasma jet is related to a specific initial bubble size selection by the TCB process that is associated with the bubbles' resonance coupling to the acoustic field [9]. The plasma jet short confinement time, its high velocity in the range of 20 Km/s, its structure much like a marline-spike, its probable ion mass separation, and its stability before and during implantation make this a very efficient implantation process for those jets near the target foil.

CLUSTERED D^+ (DD FUSION ENVIRONMENT)

The implanted $D^+ \leftrightarrow$ D 13.5 eV is a reversible conversion in target foils. See Fig. 6 A. As the dense plasma of deuterons, deuterium atoms, and electrons (10^{11}) implant into the target lattice, a coulombic charge separation between deuterons and electrons created by their different implantation range impress immediate coulombic forces that act on this coupled system. In the jet plasma there is a mixture of D^+ and D depending on the plasma temperature. The species in the implant plasma are in an exchange equilibrium ($D^+ + e^- \leftrightarrow$ D) and depend on the temperature of the plasma for the relative abundance of D^+. The D atoms entering the Pd lattice upon impact may be stripped of their electrons so mostly D^+ is implanted. In the matrix of the target surface the metallic grains (crystal boundaries and metallic crystals) will respond differently to jet implantation. The boundary region is rubble lattice and the crystal grain is a pure lattice so implantation is more predictable. The complexities of the jet plasma impact volume will be discussed in the appendix. The speculation during a lattice implant is that the electron coulombic attraction to the exterior ions of the clustered D^+ creates a situation where the mobile e^- rush to the D^+ cluster. The exterior D^+s in the cluster are converted to Ds which act as a temporary barrier to D^+ diffusion and coulombic repulsion. After some of the accelerated electrons combine with the D^+ to form D atoms with an exothermic heat input of 13.5 eV, there is, for an instant, some squeeze compression for the clustered D^+ blocking coulombic repulsion and diffusion. The heat pulse does not affect the internal D^+ cluster as DD fusion is over before the heat pulse of $D^+ + e^- \rightarrow$ D arrives at its center. (There is also within the Pd lattice a drive to convert diffusing D to D^+ which reverses the above exothermic reaction of a 13.5 eV endothermic reaction.) The volume of implantation is no longer a Pd lattice but a transient entity of D^+ cluster with some Pd atoms. A close examination of the D^+ cluster indicates that the coulombic repulsion between the centrally clustered deuterons initially cancel each other (the coulombic repulsion is equalized in the midst of the D^+ cluster). The D^+ cluster deteriorates from its outside to its interior center. The D^+ clusters may be (or not) fragmented into mini-clusters where a/some fusion event(s) may occur. In figure 6A 3→3' the DD fusion event, in the D^+ cluster that produces a fusion heat pulse removes all lattice in the vicinity as ejecta into the cavitating water. If there is no DD fusion event, then the conversion will reach its natural end with D^+ diffusing into the lattice, D converting to D^+, and the finally D^+ converts to D as it

leaves the target foil returning to D2O. The ejecta include products of fusion, the remains of the D^+ cluster, and the liquid/vapor target foil.

The time frame for coulombic interactions to operate in their nm volume, 10^6 nm^3, environment is a picosecond. The electrons, which are more mobile than deuterons, move to the trapped cluster of D^+ (3648 times more massive than e^-) converting D^+ to D. The lattice locale where this process of creating the D^+ cluster occurs is no longer part of the lattice but is an assembly of excited state atoms dominated by the D^+ ions. In the jet plasma impact or implant zone there are few Pd lattice atoms. A ratio of about 10^9 Pd/10^{11} D^+ initially exists, about equal in mass, before the DD event. The relatively slow rate of a generated D^+ conversion to a D and its heat pulse, near the velocity of sound, and surrounds the D^+ cluster with a heat pulse compression shock wave environment. This provides enough contact time for DD fusion to occur in the dense coherent cluster with heat dissipation instead of gamma radiation. As the more mobile e^- encounter the D^+ cluster, the more Ds are surrounding the diminishing D^+ in the exterior of the cluster and more heat is pumped into its surroundings. The diffusing D that just gave up its 13.5 eV to the impact zone will convert back to D^+ [10] as it moves to the Pd lattice. As Ds are produced they can also exchange their e^- with D^+. The clustered D^+s + Ds have a maximum of 10^{11} particles (probably in the order of 10^{10}) that potentially produce a 13.5 exothermic eV/event and a maximum broad heat pulse of 2.16×10^{-8} J. It is my guess that only a small portion of D^+ will convert before the DD fusion event occurs that initiates the narrow heat pulse and ejection cycle. The DD fusion events destroy the D+ clusters. See figure 6 A. The heat pulse of D^+ conversions is broad compared to the DD fusion that is initially a narrow heat pulse. . This information allows for all the ejecta sites to be considered as originating from DD fusion events.

The ejecta implant heat pulse, from a fusion event in the target foil, for a single DD fusion event is about 3.8×10^{-12} J (24 MeV) and for 10^4 fusion events is 3.8×10^{-8} J. The ejecta site population distribution according to ejecta size relates to the energy associated with each ejecta site. The total mass of target foil that may be converted to ejecta can be as high as 1/2 the mass of the target foil for long cavitation exposures. SEM photos indicate activity on both sides of the 100 μm target foil. TCB activity is attracted to the increasing number of target surface defects produced by the piezo driven acoustic input. This is demonstrated in several videos of target foils taken during exposure of target foils to the cavitation process and by visual observation of exposed target foils.

COMPARISON OF FOIL DAMAGE

After making a survey of the energies involved in the deterioration of target foils, a comparison is made of these energies. First the 1μm particles held by TCB surface tension forces as it is exported into a plasma jet are the most energetic events, near 10^{-7} J per impact event. See figure 1. These are not common but do add to the foil destruction.

The implantation process of the jet plasma appears to melt the surface layer of the target probably with most of the jet's large ions (Ar and O) impacting the target surface without penetration or stripping. The front end of the plasma (D^+ and e^-) implants into the target foil but D^+ and e^- are separated by their different ranges where the mobile implanted e^- driven by coulombic forces are captured by the exterior D^+ in the cluster to form D and 13.5 eV. There is a

heat pulse associated with this conversion. Ds do not exist long in the Pd lattice and revert to D^+s and – 13.5 eV and complete the conversion energy cycle with little net energy change. The energy in Joules for a conversion event is 2.16×10^{-18} J. The implantation impact energy is centered at 4×10^{-7} J equivalent to a 2000 nm ejecta site diameter. This is the result of a TCB selection process controlled by the temperature, pressure, and acoustic input parameters. The vent size corresponding to the energy of implant is uncommon in the SEM photos and in figure 7. The high frequency implantation shows no detected contribution from the TCB jet plasma implant to the ejecta size of around 2000 nm.

The major contribution to the destruction of foils is the DD fusion process. The heat pulse that is generated from DD fusion in the D^+ cluster upon reaching the foil surface ejects vaporous and/or liquid Pd (target foil) into the water creating an ejecta site that is observed by SEM. The number of fusion events may vary from 0 to a million for each TCB jet plasma implant and results in the formation of a transient D^+ cluster. The SEM vent site population with respect to the diameter of the site is shown in figure 7. The energy of one event is 24 MeV or 3.8×10^{-12} J and for 10^5 events is 3.8×10^{-7} J. See figure 6 B.

SUMMARY

There are two causes for target foil energy damage. The first is the bombardment of the foil with 1μm particles generated from the implantation process. See SEM photos. This bombardment from particles trapped by surface tension in the accelerating jet is similar to micro-meteor impacts. More on this phenomenon is found in the appendix of this paper. The second cause for damage is the total D^+ implantation process involving impact, charge separation, D^+ cluster and DD fusion, and heat pulse that rushes to the surface ejecting the vapor/liquid target foil into the cavitating water. See figure 6 A. There are three energy sources from the implanting process of a TCB jet into a volume of less than 0.01 μm^3 of the target foil that need to be examined. The transient change of species in that volume during implant prior to the DD fusion event is the creation path to a DD fusion environment. The three energy sources are implantation, conversion, and fusion. The first is implantation - a jet formed from a collapsing cavitation bubble is implanted into a target foil (along with a million others in one acoustic cycle) implanting D^+ and e^- into a very small volume. The second is conversion – the initially separate D^+ and e^- interact to form D on the periphery of the D^+ cluster and 13.5 eV per conversion in a broad heat pulse. The D in the Pd lattice reverts back to D^+ and – 13.5 eV cools the lattice with the result of no overall energy input. The third is fusion – a transient environment is created in the D^+ cluster that is conducive to DD fusion events. The transient environment is a D^+ cluster with a density greater than 10^{25}/cc in the center of the cluster. And coulombic forces between D^+ s in the center of the D^+ cluster on average cancel. The Maxwell tail distribution of spacing between those D^+ s allows for one or more DD fusion events to occur as disruption by the fusion heat pulse stops the fusion process. The spherical growing and energy dispersing heat pulse propagates to the target foil surface in a nanosecond where vaporized foil is propelled from the site, with the rest of the heat pulse contents, into the cavitating water. The transient events like e^- transfer, vibration motion, weak bond cleavage, and DD fusion occur in the implant volume in a picosecond time frame suggested in figures 6 and 7.

Figure 7 shows the expected narrow implant energy distribution via the implantation of a TCB plasma jet into the target foil with an impact energy of about 4×10^{-7} Joules per impact. The jet

impact is calculated from the kinetic energy plasma implant that appears to melt the surface layer of target atoms as the large ions do not penetrate, but the D^+ and e- do penetrate into the target lattice. (maybe some of the D in the plasma are stripped and also penetrate). The energy distribution is narrow because of the selection process for the TCB in the general cavitation bubble population. [9]

The upper right in figure 7 shows the point in a target foil where the implanted cluster of D^+ initiate the DD fusion events. Following the DD fusion at this point in the foil the heat pulse is initiated. The heat pulse propagates radially from the cluster reaching the surface in about a nanosecond with an eruptive burst where the liquid/vapor Pd metal, along with most of the product gases, is ejected into the water. In the calculations for DD fusion energies, the kinetic energy imparted to the target mass in the heat pulse ejected from the target (the ejecta site), are calculated values from SEM photos. Values for the mass come from the values of the ejecta volume calculated from the vent size diameters and assumed depth of one diameter. A value for the velocity of ejecta mass comes from the velocity of the heat pulse. From this, a crude evaluation for DD fusion event(s) is calculated. A site count and their diameters is made of a typical surface area of an exposed target in a SEM photo. From this ejecta site population a plot is made of the calculated ejecta site diameter and energy in Joules and MeV vs the ejecta site number in a particular diameter range. The site energies are at the bottom along the X axis and are in joules and MeV . One sees that the graph of the size distribution of sites rises to a maximum at 200 nm then falls exponentially as the vent sizes increase. The number of site diameters between 50 and 100 nanometers were in the energy range of one DD event for a jet implant and number site diameters between 100 and 200 nanometers were in the range of seven events per implant and so on. One would expect to see a maximum of around 75 nm for a single DD event. Perhaps the count is not correct because the FE SEM analysis is near the resolution limit for one event ejection or maybe it is because of a particular beneficial pre fusion grouping of D^+ in the clusters. The number of sites with 10^5 DD fusion events are rare but easily spotted in SEM photos.

The energy in DD fusion events can be related to ejecta sites which start at around 20 MeV and these counts are near a maximum event (count) number. The size of DD fusion events, that produce the SEM ejecta sites, increase in energy as they decrease in frequency (counts) exponentially.

When the measurements for any associated long range radiation were made none was found above background levels.

Acknowledgements

I would like to thank the following people who gave their time and resources to carry on this work - Mike McKubre, Fran Tanzella, Lorenza Moto, Julie Wallace, Kip Wallace, Jim Rieker, Scott Chubb, Ed Storms, Tom Claytor, Dale Tuggle, John Chandler, Dick Raymond, Richard America.

REFERENCES

[1] Kip Wallace designed an oscillator to drive the 46 KHz M 5 device. The oscillator must fit the physical dimensions of the SRI Mass Flow Calorimeter system.
[2] EQuest experiments at LANL in 1994. Invitation of Tom Claytor and Dale Tuggle.
[3] Scott Chubb,S. R. and Chubb, T. A., ICCF-8, Lerici (La Spezia), Italy, Italian Physical Society, Vol. 70, 385 (2000) -- Kim, Y., ICCF-8, Lerici (La Spezia), Italy, Italian Physical Society, Vol. 70, 375 (2000)
[4] Sonoluminescence -Reviews of Modern Physics, volume 74, April 2002; Brenner, M. P., Hilgenfeldt, S., and Lohse, D.
[5] Plasma products: Henglein, A., Ultrasonics Vol 25, 6, January (1987); D_2 and ^4He, SRI mass spectroscopy analysis by Dave Thomas 1989-1992; Reports from The U. S. Bureau.of Mines 1993 – 1994; LANL and Rocketdyne product analysis for ^4He and ^3He, Brian Oliver, 1994-5; EPRI report Fran Tanzella's mass spectroscopy analysis, 1995.
[6] Weninger, K. R., Barber, B. P., and Putterman, S. J.,Phys Rev. Lett., Vol.78, No. 9,1799 (1997).
[7] Stringham, R., ICCF-8, Lerici (La Spezia), Italy, Italian Physical Society, Vol. 70, 299 (2000)
[8] Stringham, R., ICCF-7, Vancouver Trade and Convention Center, Vancouver, British Columbia, Canada, ENECO, Inc., Poster#1, page #5 (1998)
[9] R. D. Apfel, Methods of Expermental Physics, Vol 19, 355, (Ultrasound), Edited by P. D. Edmonds, Academic Press, 1981
[10] ICCF 10, Boston - Stringham, R., ICCF-10, Boston, MA,USA, in print, (2003)
[11] Hilgenfeldt, S., Brenner, M. P., Grossmann, S., Lohse, D.,J. Fluid Mech., 365, 171 – 204 (2002)
[12] Stringham, R., ICCF-9, Tsinghua University, Beijing, China, Condensed Matter Nuclear Science, edited by Xing Z. Li Vol. 70, 323 (2002)
[13] McGraw Hill Encyclopedia of Physics, Second Edition, Ferrell, T. L., page 1051 (1993)
[14] Kantele, J, Handbook of Nuclear Spectrometry, Academic Press Limited, page 155 (1995) – Extrapolated value –

FIGURES

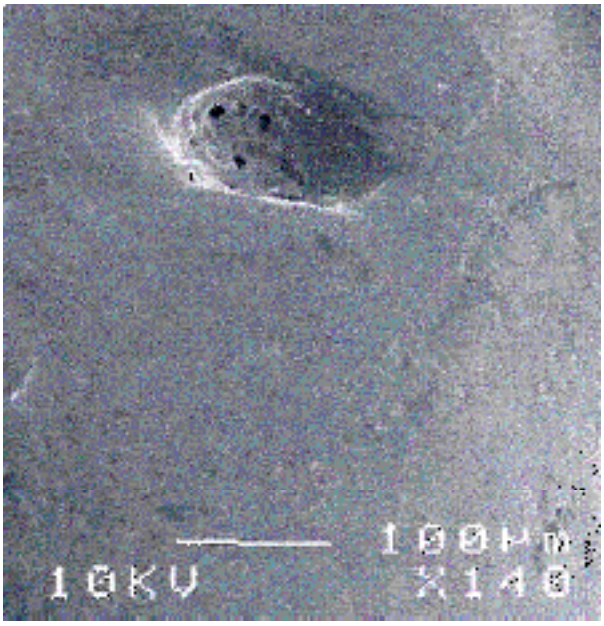

Fig. 1. SEM 100 m craters in 100µm Pd foil (M 5 reactor)

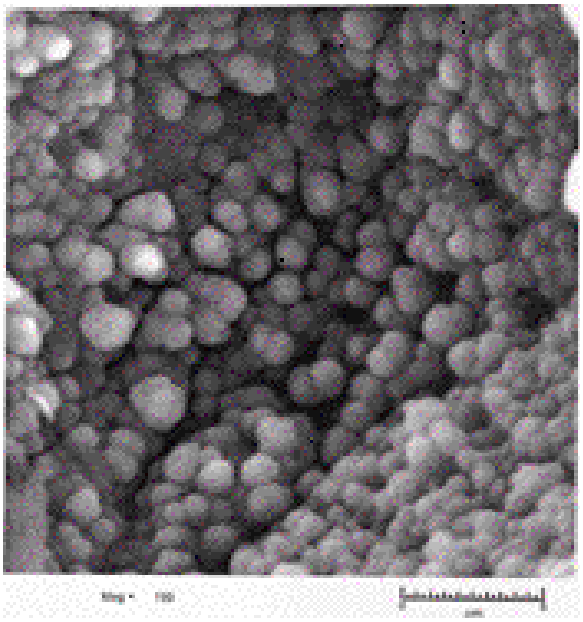

Fig. 2. SEM 1µm particles in 100µm Ag foil (M III reactor). Bar scale 5µm

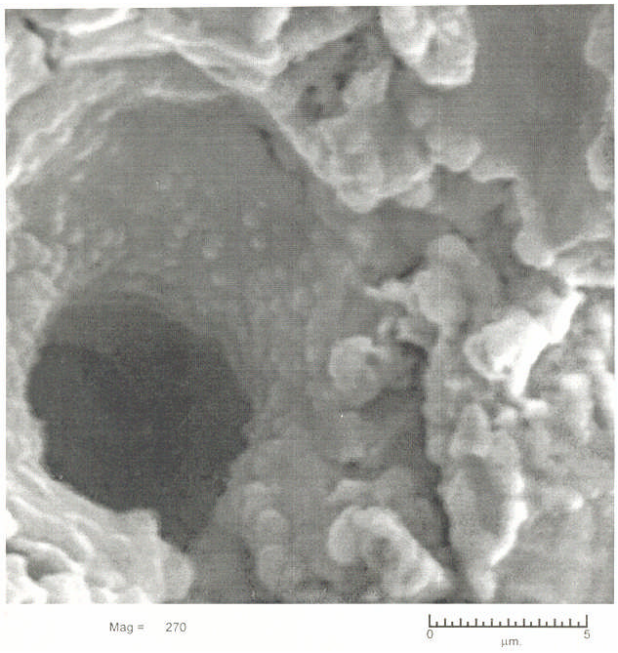

Fig. 3. SEM of exposed Ag foil ejecta site. Scale is Bar scale 5µm

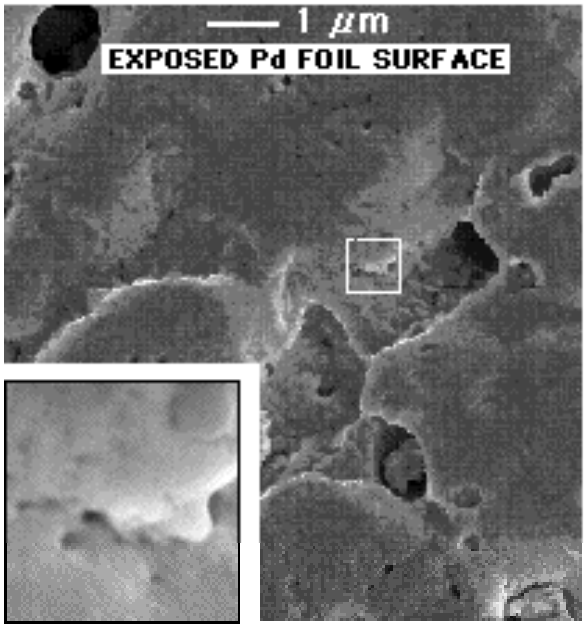

Fig. 4. SEM FE of exposed Pd foil The inset is 1 µm across.

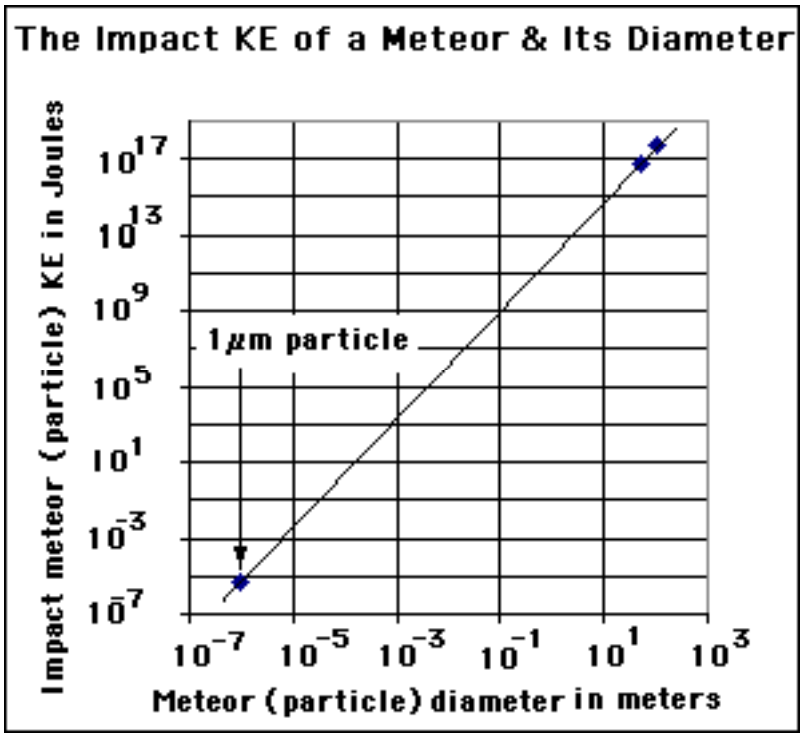

Fig. 5. A comparison of the micro particle foil impact event with the large terrestrial meteorite events to show that the scaling of impact KE and diameter of particle and meteor impacts are in reasonable agreement.

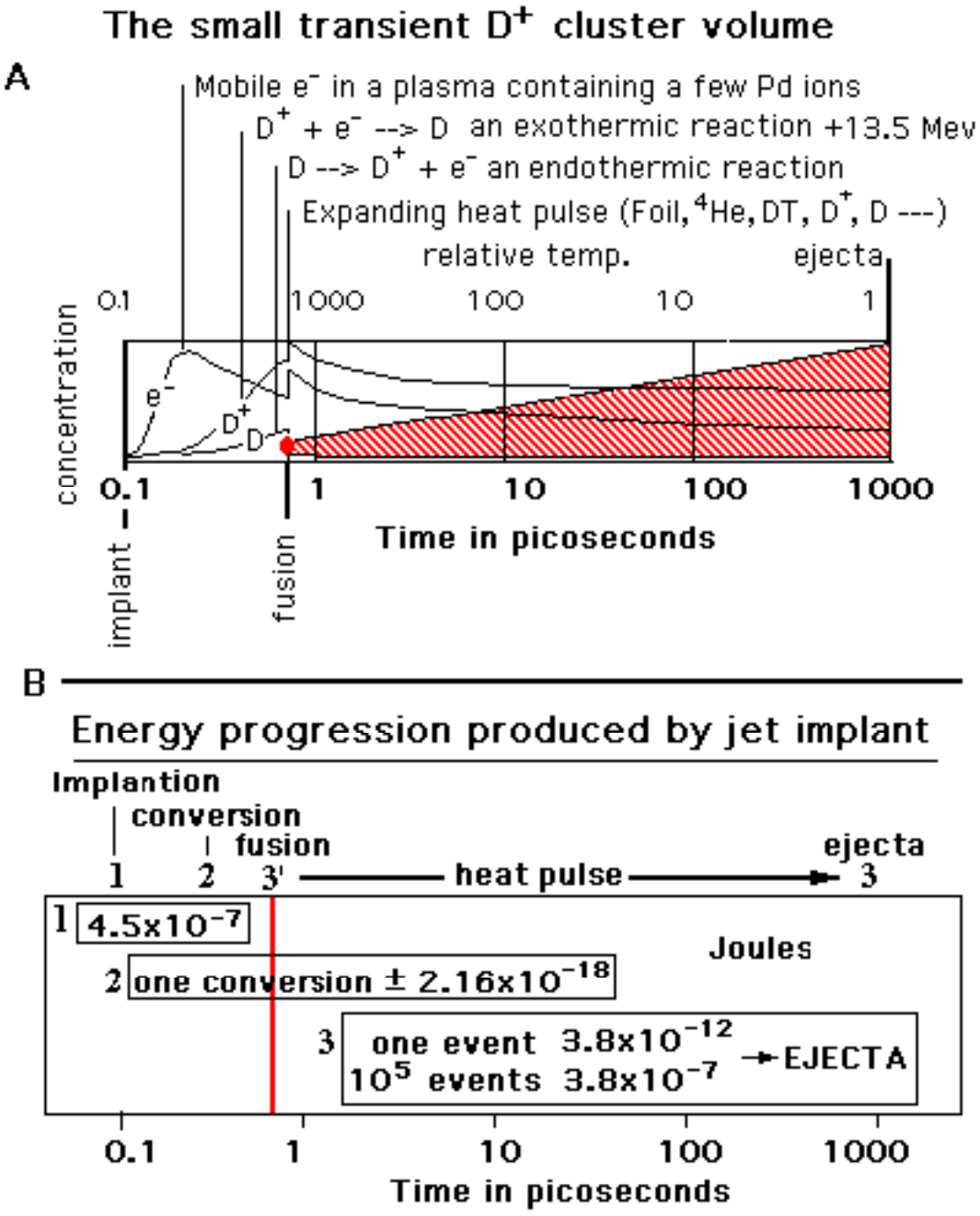

Fig. 6. The relative concentrations expected of species, during the implantation process, of D^+ + and e^- and D.

In this figure, the growth via conversions ($D^+ + e^- \leftrightarrow D$) are shown with a logarithmic time scale in picoseconds along with the log of the relative temperature. An exothermic, 13.5 eV, growth of D at the surface of the D^+ cluster is terminated with a DD fusion event. A series of conversions in the cluster of D^+ to D produces this fusion favorable environmental volume with broad heat pulse that is overwhelmed by a fusion event occurring during the first picosecond of the implantation process. At the time of spherical heat pulse initiation it moves at a velocity near Mach 1 to the target foil surface The relative temperature scale at the top of the graph shows the

decreasing temperature with increasing heat pulse volume. After about a nanosecond the heat pulse has reached the foil surface, with its high temperature and pressure, where it bursts into the cavitating water as ejecta, containing fusion products in the liquid/vapor state of the foil. The contents of the heat pulse reaching and ejecting at the surface forms the ejecta site.

Fig. 6 B shows the development of energies of the TCB jet plasma implant into a target foil.

The sorting out of energies with foil examination of ejecta sites using SEM photos indicate energetic processes occurring in target foils following jet impacts.

1 –Implantation events - With 10^{11} D^+ and D impacting the target foil with a velocity of 3×10^4 m/s produce about 5×10^{-7} Joules for each TCB implantation into a target foil.

2 – Conversion events - The exothermic $D^+ + e^- \rightarrow D$ and endothermic $D \rightarrow D^+ + e^-$ at the implant site can be viewed as a heat pulse spread over time of the entire implant fusion event, about a picosecond. The 13.5 eV exothermic and endothermic ($D+ + e^- \leftrightarrow D$) process is canceled in the long term but initially may contribute to a fusion heat pulse and the transient temperature environment of reaction volume. Only a small amount of the D conversion energy is available to use in the ejecta heat pulse at 13.5 eV per conversion event. This is a competition between conversion and coulomb repulsion.

3’ & **3** – the fusion event occurring within the D+ cluster implanted in the foil, 3’, releases a heat pulse that will travel to the foil surface in about a nanosecond ejecting vaporized foil into the cavitating water, 3. The volume of ejecta cast into the water leaves a hole in the foil surface that is photographed via SEM analysis. The population of ejection sites for a given size follows a distribution curve, shown in fig. 7, with energies varying from 3.2×10^{-12} J for one 1 DD event and to 3.2×10^{-7} joules for 10^5 events and per ejecta site.

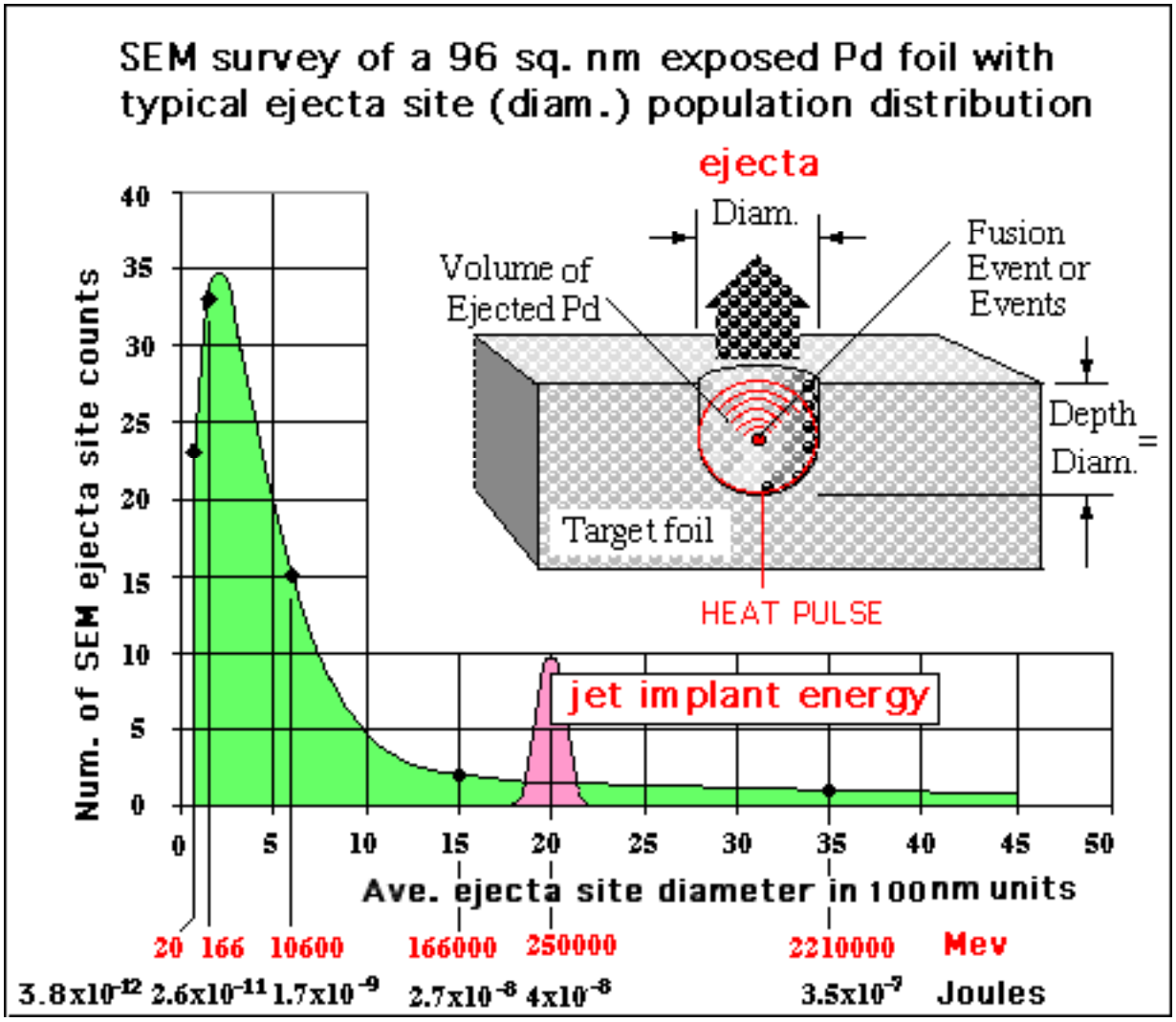

Fig, 7. SEM survey of a 96 sq. nm exposed Pd foil.

The plasma jet implant draws from a particular size in the initial TCB population and therefore, has about the same final impact energy at implant. From calculations this impact energy is about 4×10^{-8} J – purple peak. The frequency of a particular ejecta site size occurring via a size count analysis of SEM photos of Pd target foils is the key to the analysis. The energies in MeV or Joules for a particular size ejecta site correlate with the number of DD fusion events per TCB plasma jet implant into a Pd target foil. The graph shows the frequency of production of a particular size of ejecta diameter that relates to a particular number of DD fusion events. In the upper right is a cutaway view showing the result of a heat pulse and ejecta breaking the surface of a Pd target foil. The site of the fusion event and the diameter of this site indicate how the ejecta energies were calculated. The mass of ejecta depends on the number of DD events occurring in that target foil implant. From one DD fusion event expect to see about 24 MeV for one atom of ^{4}He produced, and about 48 MeV for two atoms of ^{4}He produced and so on.